Available online at www.sciencedirect.com
ScienceDirect
Journal of Solid State Chemistry 180 (2007) 213–220
JOURNAL OF SOLID STATE CHEMISTRY
www.elsevier.com/locate/jssc

Direct growth of comet-like superstructures of Au–ZnO submicron rod arrays by solvothermal soft chemistry process

Liming Shen[a], Ningzhong Bao[b,*], Kazumichi Yanagisawa[c], Yanqing Zheng[d], Kazunari Domen[e], Arunava Gupta[a], Craig A. Grimes[b]

[a]*Center for Materials for Information Technology (MINT), The University of Alabama, Tuscaloosa, AL 35487, USA*
[b]*212 Materials Research Laboratory, Department of Electrical Engineering, The Pennsylvania State University, University Park, PA 16802, USA*
[c]*Research Laboratory of Hydrothermal Chemistry, Faculty of Science, Kochi University, 2-5-1 Akebono-cho, Kochi 780-8520, Japan*
[d]*Shanghai Institute of Ceramics, Chinese Academy of Sciences, Shanghai 201800, China*
[e]*Department of Chemical System Engineering, School of Engineering, The University of Tokyo, 7-3-1 Hongo, Bunkyo-Ku, Tokyo 113-8656, Japan*

Received 5 August 2006; received in revised form 3 October 2006; accepted 9 October 2006
Available online 14 October 2006

Abstract

The synthesis, characterization and proposed growth process of a new kind of comet-like Au–ZnO superstructures are described here. This Au–ZnO superstructure was directly created by a simple and mild solvothermal reaction, dissolving the reactants of zinc acetate dihydrate and hydrogen tetrachloroaurate tetrahydrate ($HAuCl_4 \cdot 4H_2O$) in ethylenediamine and taking advantage of the lattice matching growth between definitized ZnO plane and Au plane and the natural growth habit of the ZnO rods along [001] direction in solutions. For a typical comet-like Au–ZnO superstructure, its comet head consists of one hemispherical end of a central thick ZnO rod and an outer Au–ZnO thin layer, and its comet tail consists of radially standing ZnO submicron rod arrays growing on the Au–ZnO thin layer. These ZnO rods have diameters in range of 0.2–0.5 μm, an average aspect ratio of about 10, and lengths of up to about 4 μm. The morphology, size and structure of the ZnO superstructures are dependent on the concentration of reactants and the reaction time. The $HAuCl_4 \cdot 4H_2O$ plays a key role for the solvothermal growth of the comet-like superstructure, and only are ZnO fibers obtained in absence of the $HAuCl_4 \cdot 4H_2O$. The UV–vis absorption spectrum shows two absorptions at 365–390 nm and 480–600 nm, respectively attributing to the characteristic of the ZnO wide-band semiconductor material and the surface plasmon resonance of the Au particles.

Keywords: ZnO; Solvothermal; Crystal growth; Nanomaterials

1. Introduction

Controlling the structure of inorganic semiconductor architectures remains a goal of both scientific and technological importance because these special architectures might have distinguished properties for special applications [1,2]. Zinc oxide (ZnO), as one of the most important functional materials, is a wide band gap (3.37 eV) semiconductor with a large excitation binding energy (about 60 MeV). To date, except for ZnO in forms of rod, needle and wire [3–5], some delicate ZnO superstructures, such as rotor-like [6], obelisk-like [7], tower-like and flower-like ZnO [8], have been reported. These ZnO materials, specially the superstructures of one-dimensional (1-D) ZnO arrays, could have extensively practical applications in optical, electronic and acoustic fields [9–11].

In comparison to many studies on the synthesis and property of pure ZnO materials, noble metal–ZnO composites, such as the Au (Ag or Pt)–ZnO composites, are particularly important as a typical noble metal–semiconductor for the theoretical study of the photoelectron transfer process that occurs following the creation of electron–hole pairs or excitons within the semiconductor particle [12,13]. The well-understanding of the photoelectron transfer in bulk and interface of semiconductors helps to design novel semiconductor architectures and devices for the efficient solar energy conversion. The Au (Ag or

*Corresponding author. Fax: +1814 865 6780.
E-mail addresses: nub2@psu.edu, nzh_bao@yahoo.com (N. Bao).

0022-4596/$ - see front matter © 2006 Elsevier Inc. All rights reserved.
doi:10.1016/j.jssc.2006.10.007

Pt)–ZnO composites are a kind of Schottky photochemical diodes. Moreover, ZnO is a photocatalytically active metal oxide with a strong exciton absorption band in the visible part of the spectrum. Under the illumination of light, the exciton absorption bands of ZnO [14,15] are strongly bleached by the presence of accumulated conduction band electrons because of either the Mosse–Burstein effect [16], or electric field modulated effects on the excitonic levels by trapped carriers, the so-called Stark effect [17,18]. Au (Ag or Pt) deposited on the surface of ZnO to form the metal nanostructures change the Fermi level equilibration and band structure of ZnO through storing and shuttling photogenerated electrons from the ZnO to acceptors in a photocatalytic process. By aid of some spectrum technologies, we are able to understand the electron transfer process. Thus, the efficiency of both photocatalysis and photoelectric energy conversion can be greatly improved by depositing noble metals of Pt, Ag, and Au on the surface of ZnO. Previous researches about the noble metal–ZnO composites only limited to the studied particles with simple morphology and structure. However, the morphology of ZnO and the specially organized way between noble metal and ZnO are two key factors that influence on the creation of electron–hole pairs or excitons within the ZnO particles and the subsequent photoelectron transfer process. Therefore, it would be very significant to study on how to devise simple and efficient solution method to directly create special architectures of noble metal–ZnO rod arrays firstly before we explore their properties and applications [19–22].

Various synthesis methods have been reported for preparing inorganic semiconductor superstructures, but the solution process is the simplest and most versatile synthetic approach by which many kinds of materials have been prepared under mild conditions in a large scale with low cost. By aid of some experimental results and materials growth habits, the researchers have designed one-step or multi-step procedures for growing the superstructures of ZnO rod arrays in solution conditions [22–25], such as the creation of attractive ZnO rod arrays on conducting glass substrates in aqueous solution [1,22], a two-step ZnO-seeded growth of ZnO nanowire arrays on silicon wafers in aqueous solution [2], and a low-temperature, solution-based approach for preparing complex and oriented ZnO nanostructures [25].

The solvothermal soft chemical process is a widely used solution method for preparing materials with specially controlled structures. The ethylenediamine or other amines were widely employed to act as "a shape controller" in the solvothermal synthesis of various semiconductor nanowires/nanorods [26]. ZnO with various morphologies was prepared by the amine-aided solvothermal hydrolysis of zinc acetate hydrate [27,28]. Meanwhile, ZnO nanorods can also grow from ZnO nanoparticles or clusters in solution by aid of the natural growth habit of the ZnO rods along [001] direction [29]. Further, Au nanoparticles can be prepared by converting $Au(amine)_2^{3+}$ complex through the amine mediate solvothermal reduction [30–32]. ZnO nanowires and nanorods also can grow on the Au film [33,34]. The above experimental phenomena and results remind us whether it is possible to develop a simple and efficient solution procedure to prepare attractive Au–ZnO superstructures at moderate temperature, template-free or substrate-free conditions, taking advantage of the lattice matching growth between definitized ZnO plane and Au plane and the natural growth habit of the ZnO rods along [001] direction in solutions. Here, we demonstrate a one-step solvothermal growth of novel comet-like superstructures of Au–ZnO rod arrays from reactants of zinc acetate dihydrate and hydrogen tetrachloroaurate tetrahydrate in ethylenediamine at mild temperature without any templates or substrates.

2. Experimental section

Materials: Zinc acetate dihydrate (>99.9% purity, $Zn(CH_3COO)_2 \cdot 2H_2O$), hydrogen tetrachloroaurate tetrahydrate (>99.9% purity, $HAuCl_4 \cdot 4H_2O$), ethylenediamine (>99.9% purity, $H_2N(CH_2)NH_2$), and ethanol (dehydrated, 99.5%, C_2H_5OH) were obtained from Wako Pure Chemical Industries, Ltd. 2 wt% $HAuCl_4$ ethanol solution was prepared by dissolving the $HAuCl_4 \cdot 4H_2O$ in ethanol. All chemicals were used as received.

Synthesis: In a typical synthesis of comet-like superstructures of radially standing ZnO submicron rod arrays, 0.3 g of zinc acetate dihydrate and 0.3 g of 2 wt% $HAuCl_4$ ethanol solution were mixed in 25 ml of ethylenediamine in a Teflon-lined stainless-steel autoclave. After sealing, the autoclave was heated at 160 °C for 24 h and then cooled to the room temperature. A little amount of precipitate was collected, washed with distilled water and ethanol several times, centrifuged and then dried in a vacuum oven at 50 °C. Compared with the above typical procedure, the formation process of this comet-like ZnO superstructure was also studied by controlling the reaction time at 6 and 12 h, respectively. Further, the influence of the concentration of reactants on the morphologies and structures of products was also investigated.

Characterization: Powder X-ray diffraction (XRD) patterns were recorded on a Rigaku Rotaflex Type X-ray diffractometer. Cu$K\alpha$ radiation ($\lambda = 1.5405$ Å) with a nickel filter was used, operating at 40 kV and 100 mA. All powder samples were measured in the continuous scan mode at 30–80° (2θ) with a scanning rate of 0.02° (2θ)/s. Peak positions and their relative intensities of products were characterized by comparing to Joint Committee for Powder Diffraction Standards (JCPDS). The morphologies and structures of products were observed via Scanning Electron Microscope (SEM, S-350, Hitachi Ltd., Japan) and Transmission Electron Microscopy (TEM, JEM 2010, JEOL, Japan), equipped with Energy Dispersive Spectroscopy (EDS) spectra and Select-Area Electron Diffraction (SAED). Ultraviolet–Visible diffuse reflectance spectra (UV-Vis DRS) were obtained on a V-560, JASCO.

3. Results and discussion

3.1. Morphology, structure, and optical adsorption property of typical comet-like Au–ZnO superstructures

Fig. 1 shows the XRD pattern of products prepared in the typical synthesis procedure. All main peaks in this pattern are strong and can be indexed as a hexagonal phase of zinc oxide (space group $P6_3mc$, wurtzite structure, a: 3.2498 Å; c: 5.2066 Å JSPDS card No. 36-1451). The cell parameters of a and c of as-synthesized sample,respectively,are 3.2537 and 5.2184 Å, that are very close to the standard values. In addition to the peaks of ZnO, three weak diffraction peaks, attributing to Au (111), Au (200) and Au (222) planes, are also observed (JSPDS card No. 04-0784). No peaks belonging to other chemicals are found. These indicate that zinc acetate dihydrate and $HAuCl_4$ decompose respectively to form ZnO and Au through the ethylenediamine-assisted solvothermal reaction. Further, the mole ratio of Au/Zn in starting reactants is much small, so correspondingly, the mole ratio of Au/ZnO in the products is much small, too. Therefore, the peak intensity of Au is weaker than that of ZnO.

The morphology and structure of the product were investigated by SEM. Fig. 2a shows an overall SEM image of Au–ZnO comet-like superstructures. Most products are composed of a thick rod in the center of the comet structure, a crown growing around one end of the centrally thick rod and many smaller and thinner rods protruding out from the crown, forming special comet-like superstructures. Indeed, the yield of this kind of superstructures is very high. The superstructures usually have regular comet-like morphology and process lengths of up to 10 μm The head of comet-like superstructures is composed of a hemispherical end of the central thick ZnO rods with diameters in range of 2–3 μm, and this hemispherical end is partly covered by an Au–ZnO thin layer, as shown in the SEM image of Fig. 2a, which is confirmed by the subsequent HRTEM characterization. Herein, the head of comet-like superstructures has total diameters in range of 4–6 μm. For each comet-like superstructure, the unusual standing ZnO rod arrays grew radially from one center crown on its head. Fig. 2b, a side-view SEM image of a typical superstructure, shows a central thick ZnO rod and all other surrounding protrudent ZnO rods with diameters varying from under 0.1–4 μm growing on the Au–ZnO thin layer. With increasing the distance to the central thick ZnO rod, the diameters and lengths of these ZnO rods, respectively, become smaller and shorter, which is due that the edge of the Au–ZnO thin layer and the ZnO rods growing on it are formed at the later reaction stage and process shorter growth time.

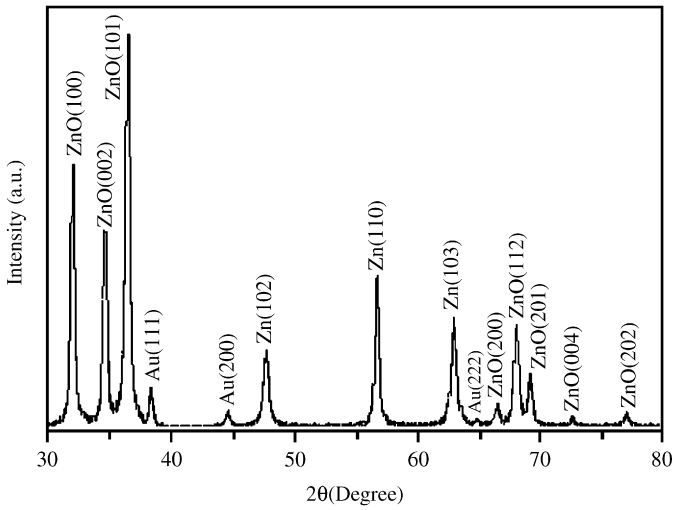

Fig. 1. XRD pattern of typical comet-like ZnO superstructures.

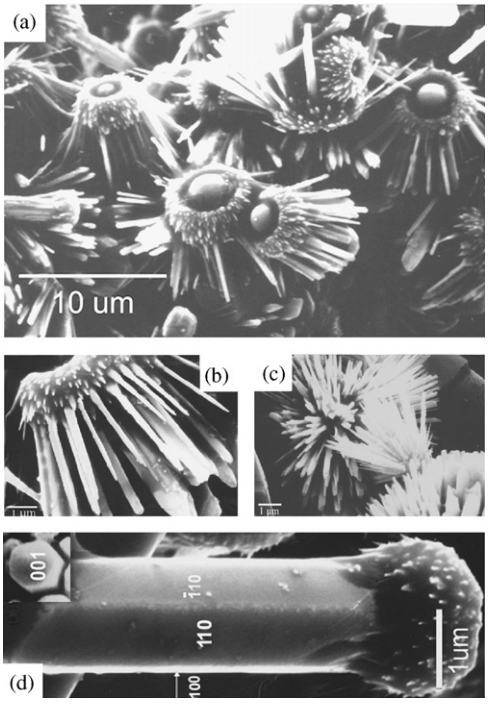

Fig. 2. SEM images (a) of the comet-like Au–ZnO superstructures on large scale, (b) side-view of a comet-like Au–ZnO superstructure, (c) a sea-urchin-like superstructure, and (d) a regular prismatic ZnO rod with hexagonal cross section (the inset).

A few special aggregates with different morphologies were also found in the product. Fig. 2c shows a sea urchin-like particle with many needle-like ZnO rods consisting of ZnO rods with uniform diameters ranging from 200 to 500 nm, lengths of up to several micrometers, and an average aspect (length/diameter) ratio of around 10. Under some special growth conditions, the ZnO rods at the center of the Au–ZnO thin layer growing at a relatively high speed, might limit the growth of other ZnO rods on the Au–ZnO thin layer. Consequently, it is possible to obtain a large single crystal of a regularly hexagonal prism ZnO rod processing a hexagonal cross section, as shown in the inset of Fig. 2d. This is supposed to be the original morphology of the central rod without any influence of surrounding slim rods during its growth. The hexagonal cross section of

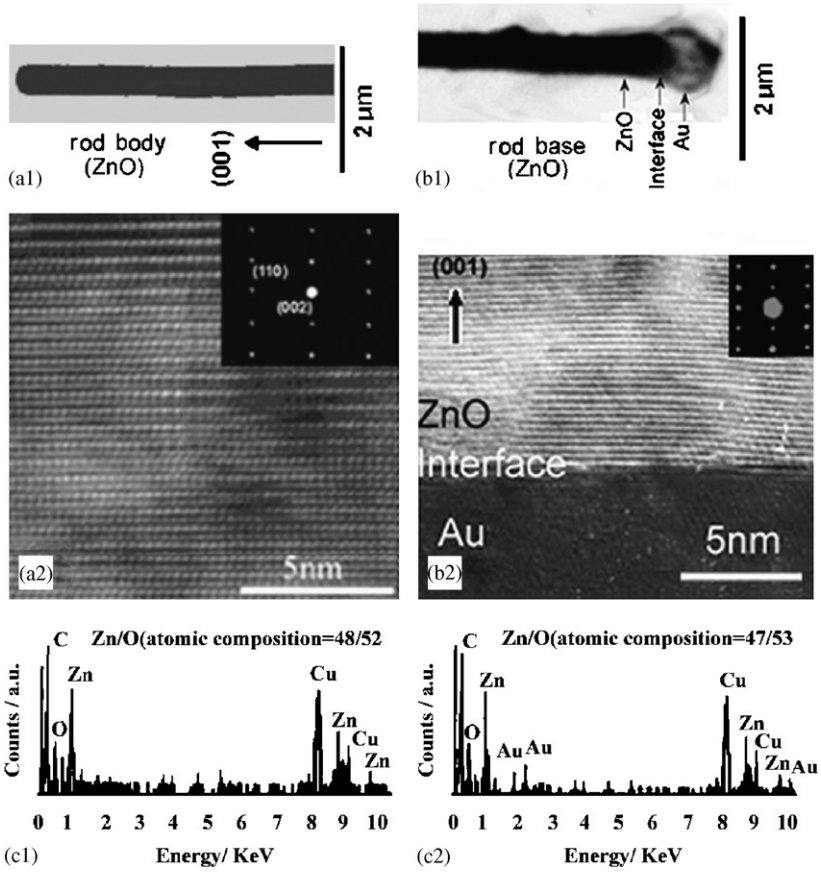

Fig. 3. TEM (a1) and HRTEM (a2) images of the body of an exfoliated ZnO rod; TEM (b1) and HRTEM (b2) images of the growth base of the same exfoliated ZnO rod; EDS spectra of (c1) the body and (c2) the growth base of the ZnO rod.

the ZnO rod clearly shows the (001) plane and indicates the [001] growth direction of ZnO rods.

Further details about the ZnO rods on the comet tail of Au–ZnO superstrutures including the morphology, composition and structure were studied by TEM, EDS, and SAED. Fig. 3(a1) clearly shows the body of ZnO rod with a hemispherical end. Fig. 3(b1) shows the morphologies of the growth base of one fine ZnO rod exfoliated from the Au–ZnO thin layer. HRTEM images of the body and the growth base of the ZnO rod are, respectively, shown in Fig. 3(a2) and (b2). It was found that the crystal planes, perpendicular to the rod axis, on the whole ZnO rod have the same lattice spacing of 2.59 Å, which corresponds to the distance between two adjacent (002) planes of the hexagonal ZnO. This indicates the preferred [001] growth direction of ZnO rods. Corresponding SAED patterns of the whole ZnO rod (the insets in both Fig. 3(a2) and (b2)) display strong ordered electron spots, and the SAED patterns taken from various parts of the ZnO rod show exactly the same pattern without further tilting the rod. These confirm the ZnO rod is of single crystal structure and preferred growth direction, in agreement with the HRTEM results. No dislocations or stacking faults at the whole interfacial region between ZnO and Au were observed in Fig. 3(b2). So we estimate ZnO rod grows epitaxially on the certain planes of Au, taking advantage of the lattice matching growth between definitized ZnO plane and Au plane. The EDS spectra of both the body, as shown in Fig. 3(c1), and the growth base, as shown in Fig. 3(c2), of the ZnO rod show nearly the same Zn/O atomic composition approaching 1, indicating the high purity of ZnO component for the whole ZnO rod. Additional Cu and C signals are contributions of the copper grid coated with porous carbon film for supporting samples. Au signal due to the Au–ZnO growth base of ZnO nanorods is detected, confirming the chemical composition of the Au–ZnO thin layer.

Fig. 4 shows the UV–Vis DRS collected from the typical Au–ZnO superstructures. The strong absorption at 365–390 nm originates from ZnO, which is the characteristic of ZnO wide-band semiconductor material. Another broad absorption band in the spectral range of 480–600 nm is due to the surface plasmon resonance of the Au particles. The Au of the Au–ZnO thin layer on the head of the comet-like superstructures is evident from their optical spectra.

The morphologic formation and structural evolution of this new kind of comet-like Au–ZnO superstructures was

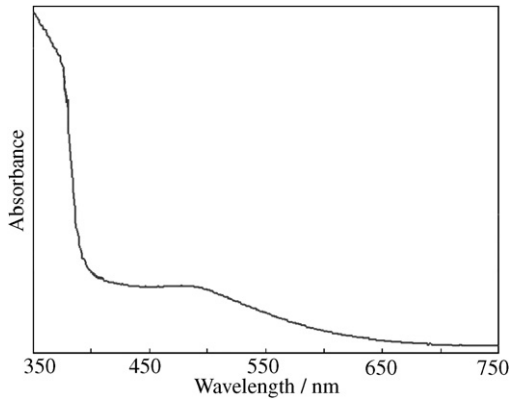

Fig. 4. UV–vis diffuse reflectance spectra of typical comet-like Au–ZnO superstructures.

also investigated through experimental designs, considering the influence of the reaction time and the concentration of reactants, as described in the following part.

3.2. Influence of the reaction time on the morphology and structure of Au–ZnO superstructures

Compared with the synthesis of typical comet-like ZnO superstructures, the morphologic change and the structural evolution of products, with changing the reaction time, was investigated by SEM. Fig. 5 shows SEM images of the products generated by solvothermal reactions at 6 and 12 h.

Fig. 5(a1–a3) show SEM images of the product formed at 6 h, keeping the same other conditions as those of the typical synthesis procedure. Fig. 5(a1) displays an SEM image of these products, showing the initial formation of the comet head and tail. Most of particles show a helianthus-like structure. A few ZnO thick rods were also observed. Fig. 5(a2) shows a bottom-view SEM image of a magnified single particle. The center is one end of a thick ZnO rod coated by an outer Au–ZnO thin layer. Fig. 5(a3) shows a side-view SEM image of a magnified single particle on which radially standing ZnO rods have grown a little over the Au–ZnO thin layer. These small ZnO rods have nonuniform diameters in range of 40–100 nm and lengths of up to 200 nm. The ZnO rods close to the edge of the Au–ZnO thin layer have slightly shorter lengths and smaller diameters.

Fig. 5(b1–b3) shows SEM images of the product formed at 12 h. Fig. 5(b1) displays particles with the morphology and structure similar to those generated at 6 h, but the whole length of the superstructure particles becomes longer. Fig. 5(b2 and b3) are bottom-view and side-view SEM images of superstructure particles, respectively. Most of products consist of a centrally thick ZnO rod and many surrounding small ZnO rods growing radially. Compared with the products formed at 6 h, larger ZnO rods have grown far above the Au–ZnO layer. With the time prolongation, highly ordered comet-like superstructures of radially standing ZnO submicron rod arrays, as shown in Fig. 2, are finally formed at 24 h.

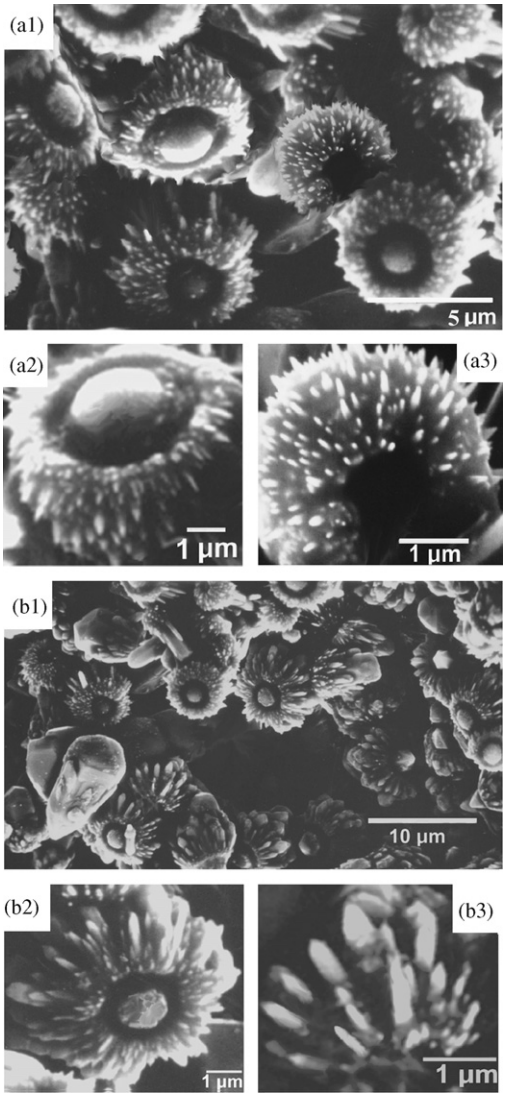

Fig. 5. SEM images (a1, a2, and a3) of the products prepared at 6 h; Side-view (a2) and bottom-view (a3) SEM images of a comet-like particle head, showing the starting growth of radially standing ZnO rod arrays; SEM images (b1, b2, and b3) of the products prepared at 12 h; Side-view (b2) and bottom-view (b3) SEM images of a comet-like particle head, showing the growth of radially standing ZnO rod arrays. All other synthesis conditions were kept the same as those of typical Au–ZnO superstructures.

3.3. Influence of the amount of reactants on the morphology and structure of Au–ZnO superstructures

The concentration of reactants is a vital factor for controlling the morphology and structure of products. In comparison to the typical synthesis procedure of the ZnO superstructures, if only was the concentration of $HAuCl_4$ largely decreased, the Au–ZnO thin layer on the head of superstructures, as shown in Fig. 6a, is too small to observe. If only was the concentration of zinc acetate doubled in the synthesis, the obtained ZnO rods becomes quite larger, and hexagonal ZnO micron rods radially stick together, as shown in Fig. 6b, which indicates that the size of ZnO rods is determined by the concentration of zinc

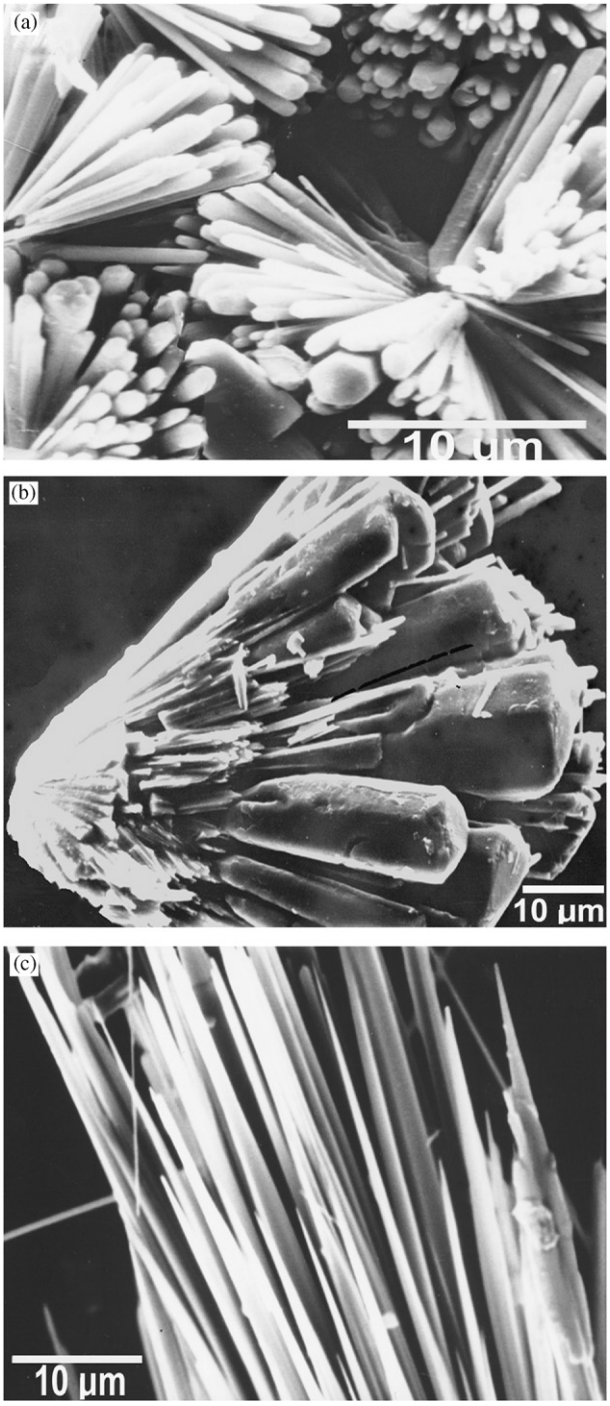

Fig. 6. SEM images of the products prepared under the conditions of (a) decreasing the amount of $HAuCl_4$ reactant to 0.05 g; (b) doubling the concentration of zinc acetate dihydrate; and (c) in absence of $HAuCl_4$ reactant. All other synthesis conditions were kept the same as those of typical Au–ZnO superstructures.

acetate in solution. This is similar to the way of decreasing the concentration of $HAuCl_4$ in the synthesis. Further, the existence of $HAuCl_4$ is undoubtedly the key factor determining the formation of the unique comet-like superstructures. If no $HAuCl_4$ was added in the synthesis while keeping the same other conditions as those of the typical procedure, only are nearly parallel ZnO fibers obtained, as shown in Fig. 6c.

3.4. Possible formation process of the comet-like Au–ZnO superstructures

Up to date, to the best of our knowledge, controlling of architecture and patterning of ZnO were done by two main methods: (1) The high-temperature VLS method for preparing ZnO of various morphologies on a layer of catalyst coating on substrates, such as the preparation of nanowires/nanobelts/nanorods on Au catalyst [3,32] or Sn catalyst [4,19,20] and rotor-like ZnO on ZnO substrates [6]; (2) Hydrothermal methods for preparing ZnO of various morphologies on various substrates, such as rotor-like ZnO grown on ZnO substrates [6], obelisk/tower/flower/tube-like ZnO nanorods grown on quartz and amorphous glass wafers [7,8], ZnO nanowires grown on various substrates (e.g., polycrystalline F-SnO_2 glass, single crystalline sapphire, Si/SiO_2 wafers, or nanostructured ZnO thin films) [20], or without any substrates, such as the growth the prism-like/sphere-like/rod-like ZnO [35].

In order to grow the present comet-like ZnO superstructures, we adeptly considered some reported experimental results. ZnO were prepared by the solvothermal hydrolysis of the zinc–amine complexes that can form from zinc salts such as zinc acetate dihydrate and zinc nitrate hexahydrate and different amines such as ammonia, hexamethylenetetramine, and ethylenediamine via hydro/solvothermal reactions [27,28]. The zinc cation is not easily hydrolysed to form the precipitation of the hydroxide except by raising the pH with a base. The Lewis base such as ethylenediamine is a kind of good ligand often used to form the $Zn(ethylenediamine)_3^{2+}$ complex with the zinc cation, and amines such as ethylenediamine will undergo slow chemical decomposition to generate OH^- ions at elevated temperature, and then the hydrolysis of the Zn^{2+} is controlled by a slow release of hydroxide from the $Zn(ethylenediamine)_3^{2+}$ complex, avoiding the fast nucleation of the ZnO. This slower nucleation velocity allows the pregenerated ZnO clusters or nanoparticles to grow into ZnO rods with a single crystal structure.

Further, the thermodynamically stable crystal structure of ZnO is wurtzite with the ionic and polar structure described as hexagonal close packing of oxygen and zinc atoms in point group $3m$ and space group $P6_3mc$ with zinc atoms in tetrahedral sites. The ZnO crystal is the stacking order of the coordination tetrahedron by sharing elements (corner, edge or face of the coordination tetrahedron). The terminal vertex of a corner of the coordination tetrahedron can still bond with three growth units; the terminal vertex of the edge of the coordination tetrahedron can still bond with two growth units; the terminal vertex of the face of the coordination tetrahedron can only band with one growth unit. So the growth rate in the [001] direction, i.e. every coordination tetrahedron has a corner present at the

interface, is the fastest; that in the [00$\bar{1}$] direction, i.e. every coordination tetrahedron has a face present at the interface, is the lowest; the growth rates in other directions are between those in above two directions. So we estimate that the interior structural characters of ZnO determine the anisotropic growth of the ZnO rods along the [001] direction, and only do the *c*-axis-oriented radially standing hexagonal ZnO submicron rod arrays tend to form finally.

Moreover, Au nanoparticles can form by the amine-reduction of Au(ethylenediamine)$_2^{3+}$ complex [30,34]. ZnO rods also can grow on the Au particles, corresponding to what was reported that under hydrothermal conditions, the interfacial energy between crystal nuclei and substrate is usually smaller than that between crystal nuclei and solutions. The lattice misfit of ZnO(0 0 1) and Au(1 1 1) is about 11%, which also gives the possibility of ZnO rods growing on the Au particles.

Although it is difficult to know exactly the synthetic mechanism of comet-like Au–ZnO superstructures, based on numerous experiments and the previous reports, the growth process consisting of three main processes was described as that (i) a few ZnO rod formed in the first step and there is no Au formed at this stage. In this stage, ZnO trends to grow into rods, as shown in Fig. 5(a1), due to the natural growth habit described above. These ZnO rods will be located in the center of each comet-like superstructure. With increasing the reaction time, they becomes thicker and longer. (ii) With increasing the reaction time, Au crystallites gradually formed and they trend to aggregate at the grain boundary of (0 0 $\bar{1}$) plane and other crystal planes at the inert end of formed ZnO rods. These grain boundary places are the most suitable place for Au particles to nucleate, due to lattice defects. These Au particles are locally crystallized or atomically ordered and some have the plane (111) of hexagonal structure appeared at the surface, which lattice matches the ZnO (001) plane with misfit of about 11%. Therefore new ZnO from the remaining Zn reactants nucleates and grows on the Au (111) surface by the epitaxial growth and forms ZnO islands, which forms the Au–ZnO layer with Au particles grown simultaneously from the remaining Au reactants. (iii) After the Au(ethylenediamine)$_2^{3+}$ complex all converts to Au, the ZnO grows continually into rods, out of Au–ZnO thin layer, as a result of natural growth habit. With increasing the reaction time, these ZnO rods becomes thicker and longer, as shown in Fig. 5(b1–b3) and (a2).

Future work is needed to investigate the growth behavior of ZnO on the Au surface under definitized solvothermal conditions and to further adjust the concentrations of zinc acetate dihydrate and $HAuCl_4$ for preparing superstructures consisting of uniform ZnO rods or other novel architectures of ZnO rods. Nevertheless, the present results indicate that the ethylenediamine–$HAuCl_4$ could be used as an effective system in the synthesis of other semiconductor superstructures.

4. Conclusion

In summary, a simple, mild and low-temperature solvothermal growth process to successfully prepare novel comet-like Au–ZnO superstructures of radially standing submicron rod arrays. This synthesis adeptly considered the respective decomposition habit of zinc acetate dihydrate and hydrogen tetrachloroaurate tetrahydrate in ethylenediamine, the lattice matching growth of ZnO rods on Au particles, and the growth habit of the ZnO crystal under solution conditions, as well as the growth rate in the [001] direction is the fastest. The reaction time and the reactant concentration are two key factors for controlling the morphologic formation and the structural evolution of the comet-like superstructures.

References

[1] L. Vayssieres, K. Keis, A. Hagfeldt, S. Lindquist, Chem. Mater. 13 (2001) 4395–4398.
[2] L.E. Greene, M. Law, J. Goldberger, F. Kim, J.C. Johnson, Y.F. Zhang, R.J. Saykally, P. Yang, Angew. Chem. Int. Ed. 42 (2003) 3031–3034.
[3] M.H. Huang, S. Mao, H. Feick, H.Q. Yan, Y.Y. Wu, H. Kind, E. Weber, R. Russo, P.D. Yang, Science 292 (2001) 1897–1899.
[4] P.X. Gao, Z.L. Wang, J. Phys. Chem. B 106 (2002) 12653–12658.
[5] D. Ledwith, S.C. Pillai, G.W. Watson, J.M. Kelly, Chem. Commun. (2004) 2294–2295.
[6] X.P. Gao, Z.F. Zheng, H.Y. Zhu, G.L. Pan, J.L. Bao, F. Wu, D.Y. Song, Chem. Commun. (2004) 1428–1429.
[7] Z. Wang, X.F. Qian, J. Yin, Z.K. Zhu, J. Solid State Chem. 177 (2004) 2144–2149.
[8] Z. Wang, X.F. Qian, J. Yin, Z.K. Zhu, Langmuir 20 (2004) 3441–3448.
[9] Z.W. Pan, Z.R. Dai, Z.L. Wang, Science 291 (2001) 1947–1949.
[10] Q.F. Shi, L.J. Rendek Jr., W.B. Cai, Da.A. Scherson, Electrochem. Solid-State Lett. 6 (2003) E35–E39.
[11] Q. Li, C. Wang, Chem. Phys. Lett. 375 (2003) 525–531.
[12] V. Subramanian, E.E. Wolf, P.V. Kamat, J. Phys. Chem. B 107 (2003) 7479–7485.
[13] A. Wood, M. Giersig, P. Mulvaney, J. Phys. Chem. B 105 (2001) 8810–8815.
[14] P.V. Kamat, B. Patrick, J. Phys. Chem. 96 (1992) 6829–6834.
[15] P. Hoyer, H. Weller, J. Phys. Chem. 99 (1995) 14096–14100.
[16] E. Burstein, Phys. Rev. 93 (1954) 632–633.
[17] E.F. Hilinski, P.A. Lucas, Y. Wang, J. Chem. Phys. 89 (1988) 3435–3441.
[18] V.L. Colvin, K.L. Cunningham, A.P. Alivisatos, J. Chem. Phys. 101 (1994) 7122–7138.
[19] Y. Ding, P.X. Gao, Z.L. Wang, J. Am. Chem. Soc. 126 (2004) 2066–2072.
[20] X.D. Wang, Y. Ding, C.J. Summers, Z.L. Wang, J. Phys. Chem. B 108 (2004) 8773–8777.
[21] C. Burda, X. Chen, R. Narayanan, M.A. El-Sayed, Chem. Rev. 105 (2005) 1025–1102.
[22] L. Vayssieres, Adv. Mater. 15 (2003) 464–466.
[23] L. Guo, Y.L. Ji, H. Xu, P. Simon, Z. Wu, J. Am. Chem. Soc. 124 (2002) 14864–14865.
[24] Z.R. Tian, J.A. Voigt, J. Liu, B. Mckenzie, M.J. Mcdermott, M.A. Rodriguez, H. Konishi, H. Xu, Nature Mater. 2 (2003) 821–826.
[25] B. Li, Y. Xie, J.X. Huang, Y. Qian, Inorg. Chem. 39 (2000) 2061–2064.
[26] J. Zhang, L. Sun, J. Yin, H. Su, C. Liao, C. Yan, Chem. Mater. 14 (2002) 4172–4177.

[27] X. Gao, X. Li, W. Yu, J. Phys. Chem. B 109 (2005) 1155–1161.
[28] W. Li, E. Shi, W. Zhong, Z. Yin, J. Cryst. Growth 203 (1999) 186–196.
[29] M. Wu, D. Chen, T. Huang, Chem. Mater. 13 (2001) 599–606.
[30] B.P. Block Jr., J.C. Bailar, J. Am. Chem. Soc. 73 (1951) 4722–4725.
[31] S. Komarneni, Current Sci. 85 (2003) 1730–1734.
[32] J.B.S. Newman, G.J. Blanchard, Langmuir 22 (2006) 5882–5887.
[33] M.H. Huang, Y.Y. Wu, H. Feich, N. Tran, E. Weber, P. Yang, Adv. Mater. 13 (2001) 113–116.
[34] X. Wang, C.J. Summers, Z.L. Wang, Nano Lett. 4 (2004) 423–426.
[35] Q. Li., V. Kumar, Y. Li, H. Zhang, T.J. Marks, R.P.H. Chang, Chem. Mater. 17 (2005) 1001–1006.